COOLING PERFORMANCE OF A MHPA@MOF BASED HYBRID PASSIVE BATTERY THERMAL MANAGEMENT SYSTEM FOR A MODULE WITH LARGE-CAPACITY PRISMATIC LITHIUM-ION BATTERY

Xuefei Gao [a], Ying Zhang [a,b,]*, Xingyue Wu [c], Ziyi Xie [a], Xinyi Lin [a], Jun Wang [a,]*

[a] School of Safety Science and Emergency Management, Wuhan University of Technology, Wuhan, China

[b] Hubei Key Laboratory of Fuel Cell, Wuhan, China

[c] Hubei University, Wuhan, China

*****Corresponding author; email: yzhang@whut.edu.cn, 3604938@qq.com

Metal-organic frameworks are beginning to be employed in the thermal management system of lithium-ion batteries because of its high water absorption and enthalpy of phase change. However, its cooling performance is only preliminarily explored used in small cylindrical cells or a single large cell. The effect on multiple large-capacity cells has not be verified yet. In this study, a micro heat pipe arrays@MIL-101(Cr) hybrid battery thermal management system is proposed, and its cooling performance of different number of battery modules at different discharge rates is studied. Experimental results show that MIL-101(Cr) is evenly distributed, and the water vapor adsorption capacity reached 1.65 g/g. The maximum temperature of the micro heat pipe arrays@MIL-101(Cr) group was 36.42°C in the experiment of the four-cell battery pack at 1C discharge rate, which was 12.98°C lower than that of the natural cooling group and 3.05°C lower than that of the micro heat pipe arrays group. With the increase of the number of cells, the maximum temperature of the battery pack rises from 43.12°C to 47.37°C, and the temperature difference rises from 1.53°C to 5.57°C at 2C discharge rate. As the discharge rate increases, the maximum temperature of the battery consisting of four cells rises from 36.42°C to 47.37°C, and the maximum temperature difference rises from 2.87°C to 5.57°C, which suggests that the current micro heat pipe arrays@MOF based battery thermal management system be combined with an active thermal management system to ensure temperature control in high-rate and multi-battery modules.

Keywords:*Lithium-ion battery; Multi-battery module; MHPA; Thermal management; MIL-101(Cr)*

1. Introduction

With the increase of carbon emissions, global warming, and the environment being polluted, the application of new energy has gradually been paid attention to[1, 2]. Lithium-ion

batteries (LIBs) are widely used in energy storage power stations, electric vehicles and other industries due to their advantages of long cycle life, no memory effect, and high energy density.[3, 4] During the operation of the battery, the temperature will continue to rise. Once the temperature is too high, the battery capacity will decay, and even serious may lead to thermal runaway, causing safety accidents.[5] The maximum safe temperature limit for LIBs is 45°C, and the safe temperature limit for temperature difference is 5°C.[6, 7] When the batteries of the battery pack are placed side by side and discharged, due to the internal reaction of the battery itself and the heat generation of the internal resistance, heat conduction and heat convection will occur between the cells, which will affect the temperature of the battery pack. If the number of batteries is large, the maximum temperature and temperature difference of the battery pack will increase[8], and the maximum temperature and temperature difference are important parameters indicators to ensure the safety of the battery[9]. Therefore, a proper thermal management system is necessary for the safe and efficient operation of the battery.

The current state of LIBs thermal management primarily consists of active cooling technology and passive cooling technology.[10] Active cooling technology is gradually being replaced by passive cooling technology due to the large amount of energy required.[11-13] Heat pipes[14, 15] are a passive heat transfer technology that is becoming increasingly popular due to its high heat transfer efficiency.[16] By miniaturizing heat pipes so that they can be as close as possible to the hot surface, a larger contact area can be obtained, and the heat caused by local heat pipes can be quickly transferred.[17] In addition, a phase change material is a substance that changes the state of matter and provides latent heat, which can absorb and release a large amount of latent heat in the process of changing the state of matter.[18, 19]Over the past few years, considerable research has been devoted to phase change materials (PCM),[20, 21] such as lauric acid and paraffin wax, which are prone to leakage and have a low thermal conductivity. In order to improve the performance of PCM, some people combine it with other materials to prevent leakage,[22] but it is found that its enthalpy decreases as a result. As a result, the discovery of novel phase change materials with increased enthalpy and safety is an urgent matter.

Metal-organic frameworks (MOFs) are a class of crystalline porous materials with periodic network structure formed by the self-assembly of metal centers (metal ions or metal clusters) and bridging organic ligands through self-assembly.[23, 24] Due to its advantages such as porousness, large specific surface area and polymetallic sites, it has attracted attention in recent years.[25-28] Its porous structure can make some MOFs absorb a large amount of water, and the liquid gas enthalpy of water can reach 2500J/g, which also solves the problem of water fluidity. Among the many MOFs materials, MIL-101(Cr) is cited for heat dissipation in electronic devices due to its high water load.[29]Wang et al.[30] used MIL-101(Cr) in electronic devices and demonstrated that it outperforms phase change materials.

Research in this area is still in its infancy. Only a few have used MIL-101(Cr) in small battery modules in combination with other materials without considering whether it is still feasible in large battery units. Xu et al.[31]proposed to combine MIL-101(Cr) with carbon foam to form an adsorption form of battery thermal management system(BTMS), which has a high energy/power density compared with traditional PCM, Tao et al.[32] combined MIL-101(Cr) with graphene oxide(GO), which has a higher moisture absorption capacity and

moisture absorption rate, Yue et al.[33] coated MIL-101(Cr) on copper foam, and the thermal conductivity of the composite absorbent was increased to 1.9 Wm-1K-1, but the above studies are used in small cylindrical batteries, Hu et al.[34] explored that MIL-101(Cr) combined with micro heat pipe arrays (MHPA) in prismatic lithium battery packs still has good cooling performance, but the battery packs used in the experiment only have two cells. In real use, most battery packs require a large number of batteries when used, so it is necessary to explore whether BTMS can control the battery temperature within a safe temperature range when the number of batteries increases.

In this study, MIL-101(Cr) with high purity and good water adsorption was successfully synthesized, and then combined with MHPA to form a thermal management system (MHPA@MIL-101(Cr)), which was used in the battery pack and discharged the battery pack under the conditions of constant temperature and humidity (25°C, 65%RH) and different discharge rates. In addition, this BTMS is used in a battery pack composed of multiple cells, and its heat dissipation effect is verified by experiments.

2. Experiments and methods

2.1 Preparation of MIL-101(Cr).

$Cr(NO_3)_3 \cdot 9H_2O$ and PTA are mixed in a ratio of 8g:1.66g, then added to 50ml of deionized water and stirred thoroughly. The fully stirred solution was transferred to a high-pressure reaction kettle, heated at a high temperature of 220°C for 8 hours, and then taken out after cooling. The resulting crude product has a large amount of unreacted PTA. To purify MIL-101(Cr) from PTA, the product is centrifuged at high speed. Due to the different densities of MIL-101(Cr) and terephthalic acid, the crude product is centrifuged into two layers, the upper layer is terephthalic acid and the lower layer is MIL-101(Cr). The material was rinsed and centrifuged several times with deionized water until there were no obvious white impurities of terephthalate.(Fig.1) Finally, the MIL-101(Cr) obtained from multiple purifications was put into an oven and dried at 100°C for 5 hours to obtain high-purity MIL-101(Cr). For further use, the lumpy object is ground into a powder for later use.

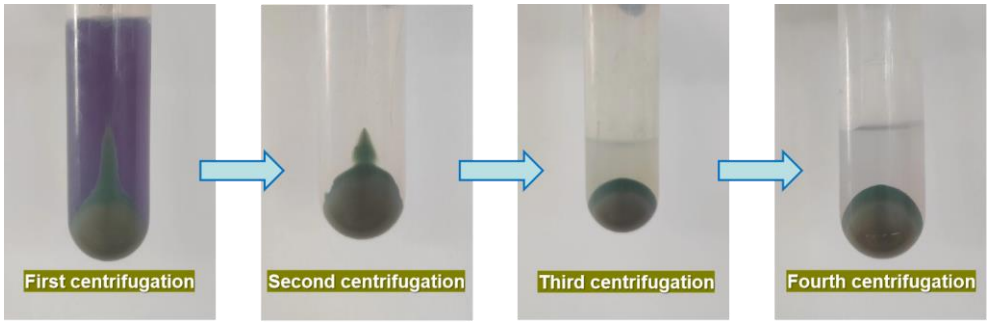

Fig. 1 MIL-101(Cr) centrifugal purification

2.2 Characterization

The surface morphology of MIL-101(Cr) were characterized using a scanning electron microscope (SEM, Tescan Mira Lms, Czech).

X-ray diffraction (XRD) patterns of MIL-101(Cr) were recorded on a D8 Advance X-ray diffractometer (Bruker D8 Advance, Germany) in the range of 5° to 60° with a scan rate of 1° min^{-1}.

The Brunauer-Emmett-Teller (BET) specific surface area and pore size distribution of MIL-101(Cr) was determined by testing the N2 adsorption-desorption characteristics in a 77K nitrogen environment with a fully automated specific surface area and pore analyzer (Quantachrome Autosorb IQ, USA). In order to verify the water absorption performance of MIL-101(Cr), the kinetic curve of water vapor adsorption-desorption of MIL-101(Cr) was tested by BET method in an environment of 298.15K.

2.3 Combination of MIL-101(Cr) and MHPA

In most previous studies on the thermal management of lithium batteries, small-capacity batteries were used to discuss the heat dissipation effect, and in order to prove that there is still a good heat dissipation effect in large-capacity batteries, this study used 66Ah ternary lithium batteries(33*180*77mm,0.98kg) for experiments. Three K-type thermocouples are evenly distributed on both sides of the battery to record the battery temperature in real time.

MIL-101(Cr) powder is dissolved in water and combined with sodium alginate in a certain proportion and applied to the condensation section of MHPA to form MHPA@MIL-101(Cr), with a general coating thickness of 1mm. A 66Ah ternary lithium battery is placed between the two MHPA@MIL-101(Cr), and the thermally conductive silica gel is covered on the contact surface between the battery and the MHPA in order to reduce the thermal resistance between the battery and the MHPA. A battery pack consisting of one cell, two cells and four cells is formed, and typically, a battery pack composed of a single cell consists of a 66Ah cell, two pieces of thermally conductive silicone, two MHPA and eight MIL-101(Cr) coatings, and the battery pack consisting of two and four cells is increased sequentially, as shown in Fig. 2.

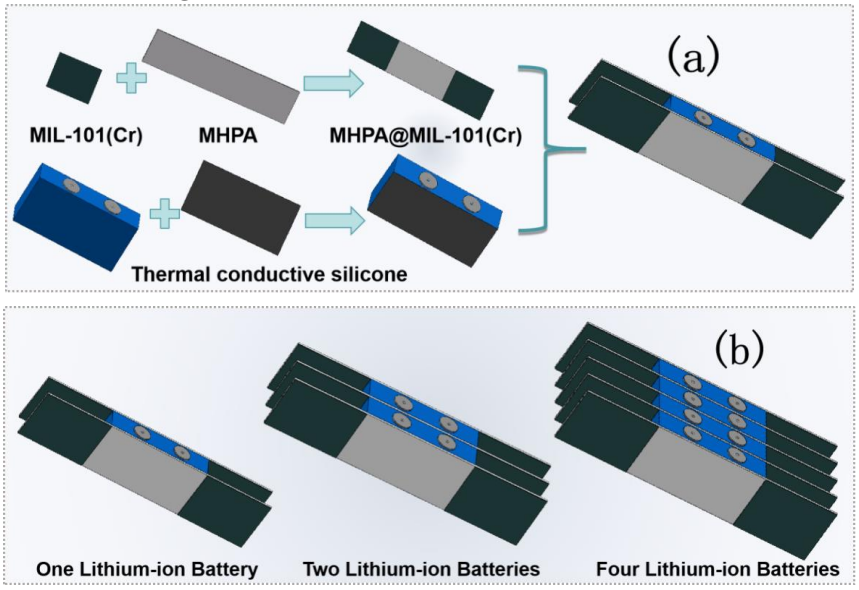

Fig. 2 (a) Composition of battery packs (b) Batteries with different quantities

2.4 Performance testing of MIL-101(Cr)(Table 1)

Tab. 1 working conditions of each experiment

Experiment	Thermal management	Number of batteries	discharge rate
#1	Natural Cooling	1	2C
#2	MHPA@MIL-101(Cr)	1	2C
#3	Natural Cooling	2	2C
#4	MHPA@MIL-101(Cr)	2	2C
#5	MHPA@MIL-101(Cr)	1	1C
#6	MHPA@MIL-101(Cr)	2	1C
#7	MHPA@MIL-101(Cr)	4	1C
#8	MHPA@MIL-101(Cr)	1	1.5C
#9	MHPA@MIL-101(Cr)	2	1.5C
#10	MHPA@MIL-101(Cr)	4	1.5C
#11	MHPA@MIL-101(Cr)	1	2C
#12	MHPA@MIL-101(Cr)	2	2C
#13	MHPA@MIL-101(Cr)	4	2C
#14	Natural Cooling	4	1C
#15	MHPA	4	1C
#16	MHPA@MIL-101(Cr)	4	1C
#17	Natural Cooling	4	1.5C
#18	MHPA	4	1.5C
#19	MHPA@MIL-101(Cr)	4	1.5C
#20	Natural Cooling	4	2C
#21	MHPA	4	2C
#22	MHPA@MIL-101(Cr)	4	2C

2.4.1 Test of MHPA@MIL-101(Cr) heat dissipation

To assess the efficacy of the BTMS(MHPA@MIL-101(Cr)), the experiments(#1,#2,#3,#4) were partitioned into two groups, one utilizing natural cooling and the other employing MHPA@MIL-101(Cr). The battery pack was discharged at a rate of 2C while maintaining the identical operating conditions (25°C, 65%RH). To facilitate a comparison of the maximum temperatures of the two groups, three thermocouples were equitably positioned on opposing sides of each cell.

2.4.2 Comparison of battery pack temperatures for different numbers of cells

To examine the impact of varying cell counts on the heat dissipation capability of BTMS, the experiment (#5-#13) was partitioned into three battery packs containing four cells, two cells and one cell, respectively, with an MHPA@MIL-101(Cr) affixed to each side of each cell within each pack. Each series-connected group of cells is placed in a box with a constant temperature and humidity of 65%RH. Under these conditions, three thermocouples are evenly distributed on both sides of each battery to determine the maximum temperature and

temperature difference of the battery pack. The three groups of batteries are discharged at rates of 1C, 1.5C, and 2C.

2.4.3 Test of the BTMS cooling performance for several cells

In order to verify the heat dissipation effect of MHPA@MIL-101(Cr) in multiple battery packs, the experiment(#14-#22) was divided into natural cooling group, MHPA group and MHPA@MIL-101(Cr) group, as shown in Fig. 3, each group of cells was composed of four 66Ah cells in series. The three battery packs were put into a constant temperature and humidity chamber respectively, and the three groups of batteries were discharged at 1C, 1.5C and 2C rates under the conditions of 25 °C and 65%RH, and the highest temperature maximum temperature and temperature difference were compared. The blank group has a 4mm gap in the middle of each battery, the MHPA group has an MHPA with no coating placed on both sides of each cell, and the MHPA@MIL-101(Cr) group has a MHPA@MIL-101(Cr) on both sides of each cell.

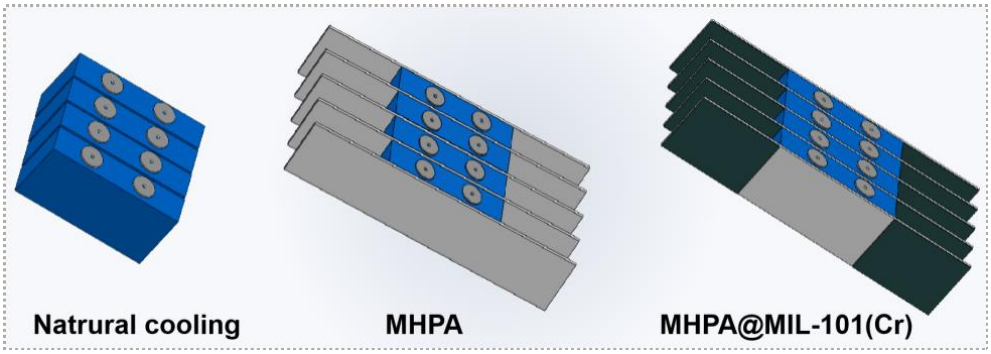

Fig. 3 Schematic diagram of the natural cooling group, MHPA group, and MHPA@MIL-101(Cr) battery pack

3. Results and discussion

MIL-101(Cr) characterization and analysis of the effect of different number of cells on the heat dissipation effect of MHPA@MIL-101(Cr), and the heat dissipation effect of MHPA@MIL-101(Cr) in multiple cells.

The evaporation section of the heat pipe contacts the battery, the working fluid absorbs heat and turns into steam, and the vapor pressure difference drives the steam from the evaporation section to the condensing section, and the MIL-101(Cr) attached to the condensing section continues to absorb heat to dissipate heat to the outside world.

3.1 Characterization test results of MIL-101(Cr)

Fig. 4 shows the XRD test plot of the synthetic MIL-101(Cr) that is in good agreement with the MIL-101(Cr) standard XRD curve simulated by the Cambridge Crystallographic Data Centre, which proves that it is MIL-101(Cr). SEM(Fig. 5) shows that the MIL-101(Cr) particles are octahedral and evenly distributed, indicating that most of the PTA has been

removed.

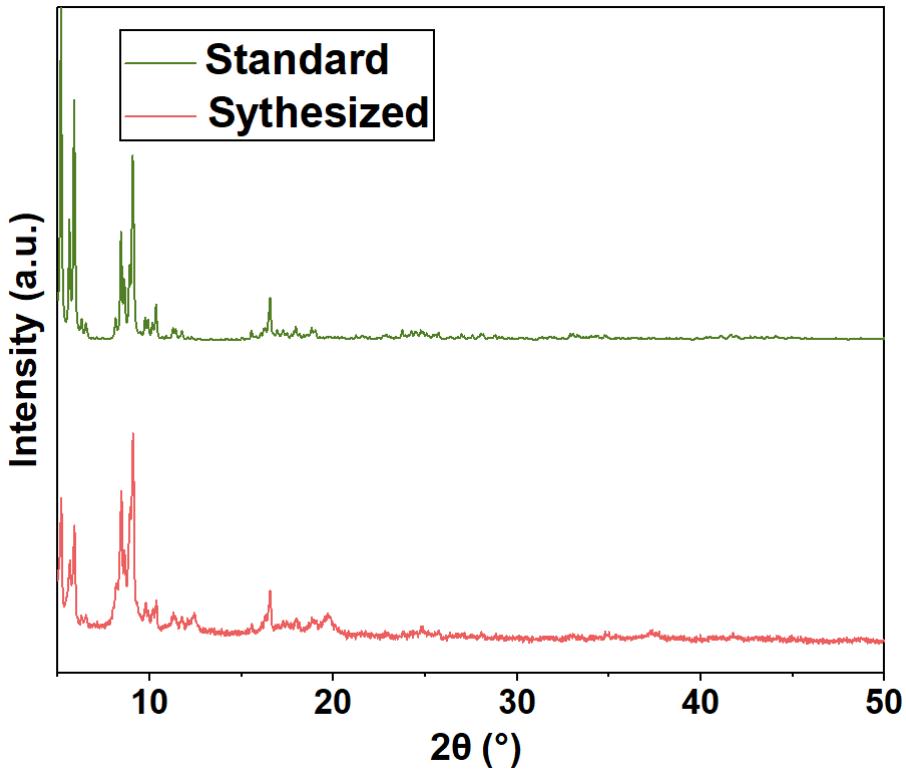

Fig. 4 XRD test results

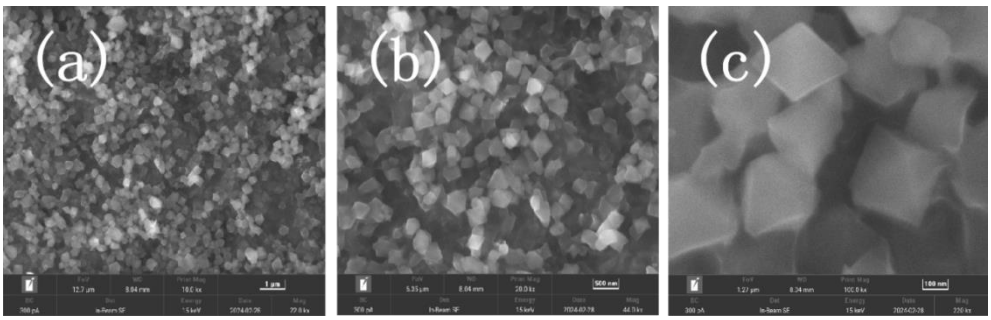

Fig. 5 SEM images of (a) 1μm , (b) 500nm and (c)100nm scale bar

According to the BET test results, the surface area of MIL-101(Cr) is 3505.146 m^2/g, the volume and area of the micropore is 1.273cm^3/g and 642.921 m^2/g, respectively. The large specific surface area and hierarchical microporous and mesoporous structure can not only provide a large number of Martian adsorption sites, but also effectively promote the rapid diffusion of ions and the rapid transfer of species. As can be seen from the adsorption-desorption curve of N_2 in Fig. 6(c), the tip adsorption curve increases sharply when the relative pressure P/P_0 is between 0-0.1, indicating the presence of a microporous structure, and the relative pressure P/P0 has a visible hysteresis cyclic isotherm within 0.3-1, indicating that MIL-101(Cr) contains mesopores. The corresponding pore size distribution curves (Fig. 6(a)) and cumulative pore volume distribution (Fig. 6(b)) obtained from the N_2 analytical data

further confirm that the material has a hierarchical micro/mesoporous structure, including two mesopores with microporous diameters of 1.2-3.5nm and 13-23nm. Water absorption is an important parameter for the performance of MIL-101(Cr), and Fig. 6(d) shows the water vapor dynamic adsorption curve, which reaches 1.65 g/g, which is higher than the water absorption of MIL-101(Cr) in some existing literature (1-1.23 g/g).[32, 33, 35, 36]

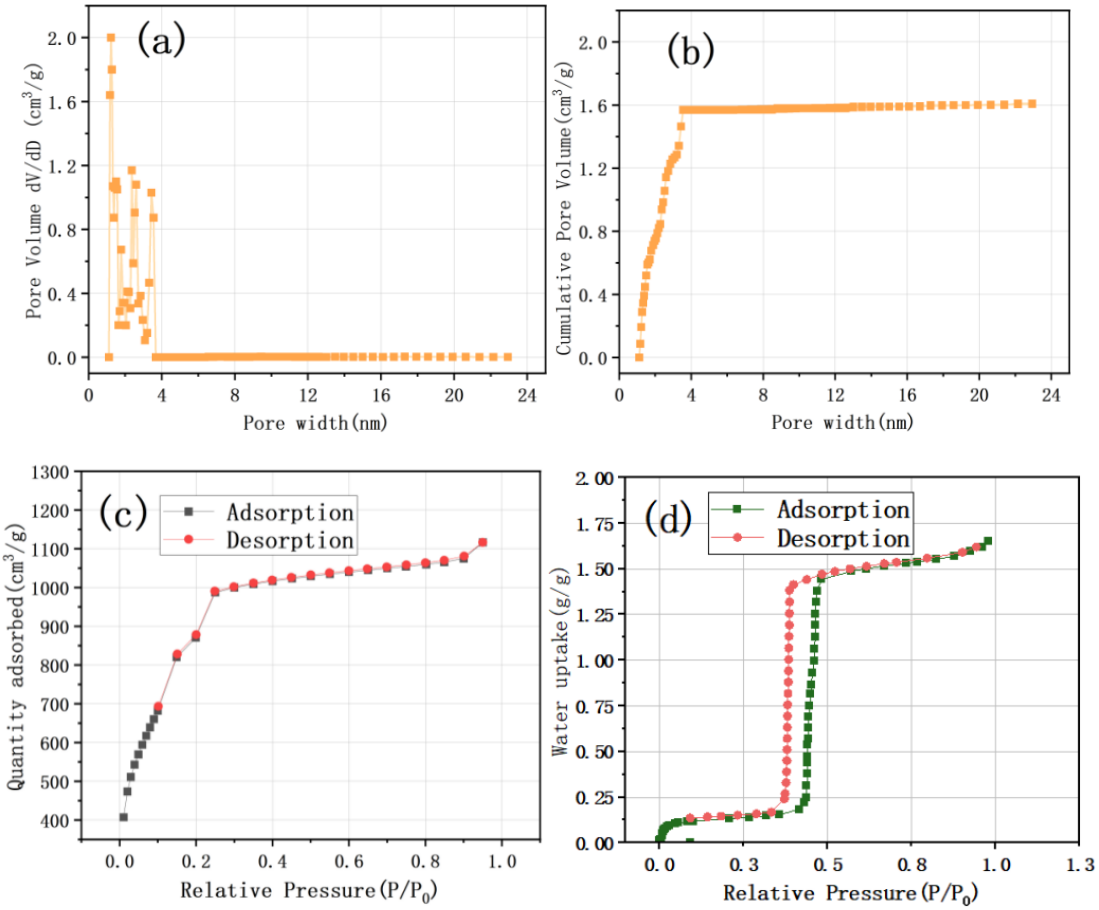

Fig. 6 (a) pore size distribution, (b) cumulative pore volume distribution, (c) N2, and (d) water vapor adsorption/desorption dynamics

3.2Heat transfer performance of MHPA@MIL-101(Cr)

As is seen from Fig. 7, MHPA@MIL-101(Cr) effectively improves the temperature characteristics of battery modules, with the maximum temperature of the natural cooling group exceeding 50°C. The maximum temperature of the MHPA@MIL-101(Cr) group was reduced to 43.12°C and 44.66°C, respectively, which did not exceed the safe temperature of 45°C, which was 9.78°C and 11.22°C lower than that of the natural cooling group, respectively, and the battery pack composed of 2 cells reduced the temperature more. As the number of cells in the battery pack increases, the battery heats up faster, the temperature difference between the evaporation section and the condensing section of MHPA is larger, and the heat transfer working fluid of the gas phase is transferred to the condensing section faster under the action of the temperature difference, so MHPA can transfer heat faster, while the dehydration phase transformation degree of MIL-101(Cr) is greater at high temperature, and the effect is more

significant. However, in reality, it is very rare to connect two batteries in series into one battery pack, and generally multiple batteries are connected in series, and the data shows that the maximum temperature of the two batteries is close to the safe temperature, which means that the feasibility of this device when multiple batteries are placed side by side in practical applications should be considered.

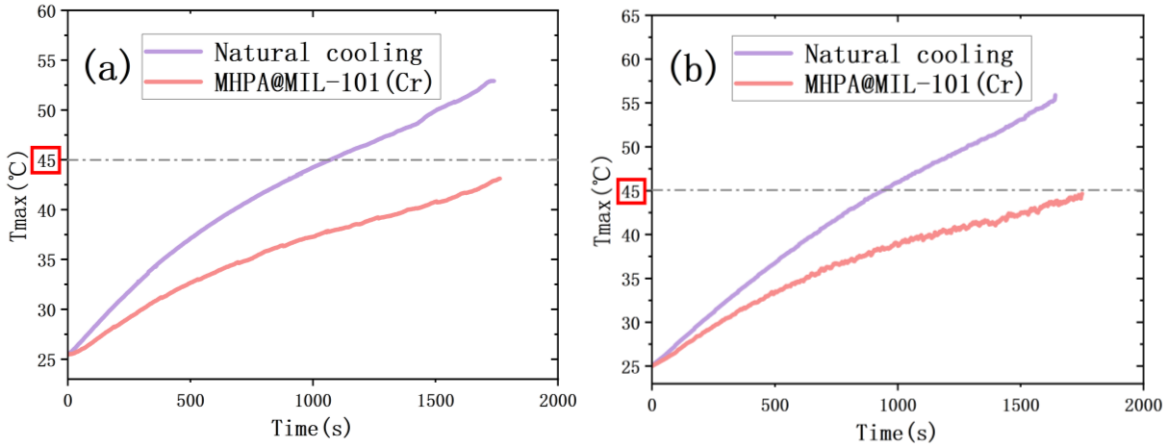

Fig. 7 (a) One cell (b) Two cells make up the maximum temperature of the battery pack

3.3 The heat dissipation effect of BTMS on different numbers of batteries

In order to verify the effect of the number of cells on the thermal management of MHPA@MIL-101(Cr), all battery packs were discharged at different rates under the same conditions (25°C, 65%RH), and the maximum temperature and temperature difference were compared. Fig. 8(a) is the change of maximum temperature of the three battery packs at a discharge rate of 1C, the curves of the three maximum temperature basically coincide before 500s, and then the three curves are separated when the temperature increases, indicating that the evaporation section of MHPA begins to absorb heat, and MIL-101(Cr) begins to dissipate heat by analyzing water. The battery pack with four cells has the highest maximum temperature, and the battery pack with two cells is in the middle, indicating that the more the number of cells is arranged, the battery's own heat increases, and the thermal boundary is poor, resulting in an increase in the temperature of the battery pack. A battery with four cells has a maximum temperature of 1.63°C higher than a two-cell pack, and a two-cell battery pack has a maximum temperature of 1.45°C higher than a single cell pack. Fig. 8(b) is the maximum temperature change curve of the three battery packs at the discharge rate of 1.5C, the maximum temperature change of the battery in the first three experimental groups basically coincides in the first 300s, and then the three curves are separated, and the upward trend becomes smaller, and the growth trend is faster than that of 1C due to the high discharge rate. The battery pack of four of the cells has a maximum temperature of 3.96°C higher than that of the two cells, and the more cells, the faster the heating rate and the higher the temperature. Fig. 8(c) is the maximum temperature change curve of the three battery packs at the discharge rate of 2C, the maximum temperature change of the cells in the three experimental groups basically coincides within 150s, due to the increase of the discharge rate, the separation time of the three curves is earlier than that of the 1C and 1.5C experimental groups, and the overall trend is

basically the same as that of 1.5C, and the upward trend of the curve will be greater than that of 1.5C. Fig. 8(d) is a line chart of the maximum temperature difference of the three battery packs at different rates, with the increase of the number of cells, the temperature difference gradually increases, and the temperature difference increases the most when discharged at 2C, which is much higher than the maximum temperature difference between 1C and 1.5C discharge rates, and the temperature difference from two cells to four cells rises more slowly than that between one cell and two cells.

In general, with the increase of the number of batteries, the maximum temperature and temperature difference of the battery pack also gradually increase, when the battery charge rate rises to 2C, the maximum temperature (47.37°C) of the battery pack composed of 4 cells has exceeded the safe temperature (45°C), and the maximum temperature difference (5.57°C) is also higher than the safe temperature difference (5°C). Therefore, it is still necessary to explore whether MHPA@MIL-101(Cr) can control the temperature of the battery pack within a safe temperature range in a battery pack composed of multiple cells.

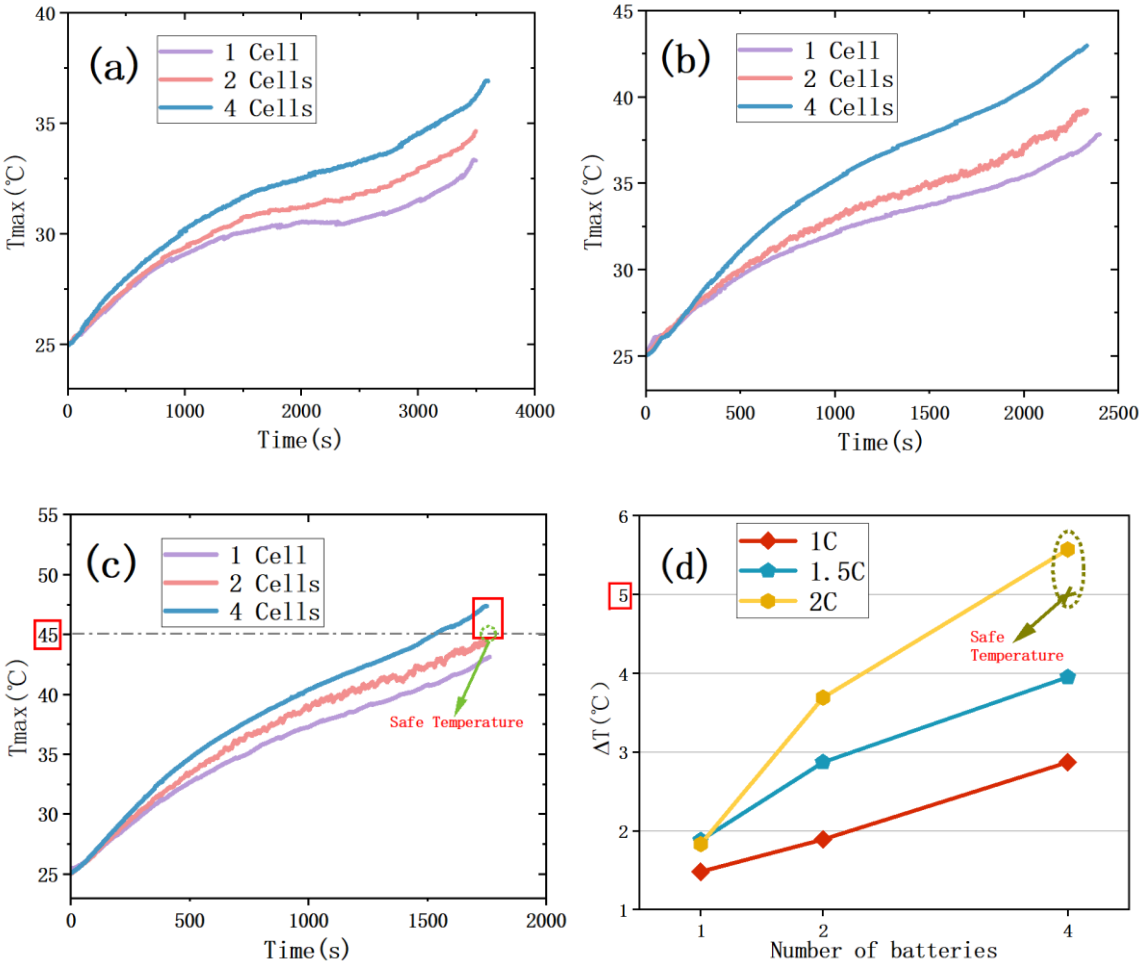

Fig. 8 Comparison of the maximum temperature at (a) 1C, (b) 1.5C, (c) 2C discharge rates, and (d) Comparison of temperature differences

3.4 Heat dissipation effect of multi-battery BTMS

In order to verify the heat dissipation effect of MHPA@MIL-101(Cr) in a multi-cell battery pack, all battery packs were discharged at different rates under the same conditions (25°C, 65%RH). Fig. 9(a) shows the maximum temperature variation of the discharge of the three battery packs at a rate of 1C. At the beginning of discharge, due to the large internal resistance, the heating rate of the natural cooling group was much greater than that of the MHPA group and the MHPA@MIL-101(Cr) group, and the temperature rise curves of the MHPA group and the MHPA@MIL-101(Cr) group basically coincided within 0-600s, and the temperature rise rate of the MHPA@MIL-101(Cr) group was significantly smaller than that of the MHPA group after 600s, which proved that MIL-101(Cr) had the effect of analyzing water. At the beginning of the 1500s, the temperature rise rate of the three groups decreased, and the temperature of the MHPA@MIL-101(Cr) group tended to be stable, and the final temperature rose due to the limited resolution rate, and the final maximum temperature was 3.05°C lower than that of the MHPA group. Fig. 9(b) is the maximum temperature change diagram of the discharge of the three battery packs at a rate of 1.5C, the battery capacity is large, the charge rate is high, the time is short, the temperature rises quickly, the temperature of the natural cooling group reaches a maximum of 54.68 °C, and the temperature curves of the MHPA group and the MHPA@MIL-101(Cr) group still basically coincide before 300s, and the maximum temperature of the final MHPA group is 45.25 °C, MHPA@MIL-101(Cr) decreased by 2.5°C compared to the maximum temperature in the MHPA group. Fig. 9(c) shows the maximum temperature variation of the discharge of the three battery packs at 2C rate. The overall trend is basically consistent with 1.5C, after 1500s, the temperature rise rate of MHPA@MIL-101(Cr) increases, and the temperature difference between the battery and the MHPA group gradually decreases, and the battery discharge heating rate accelerates, and the resolution speed of MIL-101(Cr) is limited, which decreases by 1.56°C compared with the MHPA group, and still has a significant cooling effect. Fig. 9(d) is a comparison of the maximum temperature difference between the three groups of experiments, from the natural cooling group to the MHPA group and then to the MHPA@MIL-101(Cr) group, the temperature difference gradually decreases, and the maximum temperature difference of the natural cooling group with 2C discharge reaches 15.02°C. The maximum temperature difference of the 1C discharge MHPA group was 3.45°C lower than that of the natural cooling group, and the maximum temperature difference of the MHPA@MIL-101(Cr) group was 1.58°C lower than that of the MHPA group. The maximum temperature difference of the MHPA group discharged at 1.5C was 3.71°C lower than that of the natural cooling group, and the maximum temperature difference of the MHPA@MIL-101(Cr) group was 2.61°C lower than that of the MHPA group. The maximum temperature difference of the MHPA group discharged at 2C was 7.7 °C lower than that of the natural cooling group, and the maximum temperature difference of the MHPA@MIL-101(Cr) group was 1.75°C lower than that of the MHPA group.

In general, in the four-cell battery pack, MHPA@MIL-101(Cr) still has a significant cooling effect compared with the natural cooling group and the MHPA group, and the maximum temperature of the MHPA group (45.25°C) is near the safe temperature when discharged at 1.5C, and the temperature can be reduced to below 45°C in the

MHPA@MIL-101(Cr) group. Only when the maximum temperature and temperature difference of the battery pack cannot reach the safe range when the battery is discharged at 2C, the battery pack temperature can still be controlled within the ideal temperature under normal charging and discharging.

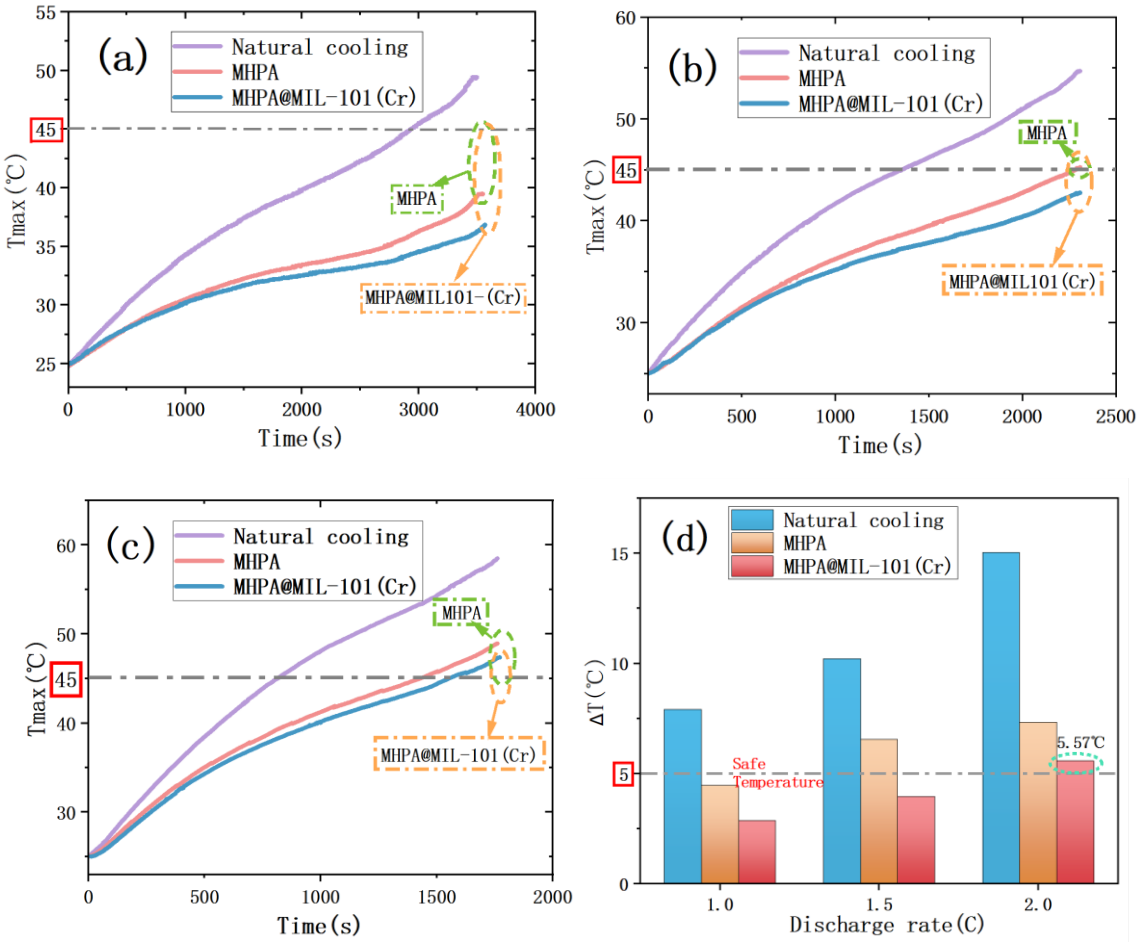

Fig. 9 Comparison of the maximum temperature of the battery pack at 1C(a), 1.5C(b) and 2C(c) discharge rates,(d) Comparison of temperature difference of battery modules.

The above two experiments were compared with the highest temperatures at 1C, 1.5C, and 2C discharge rates. (Fig.10)

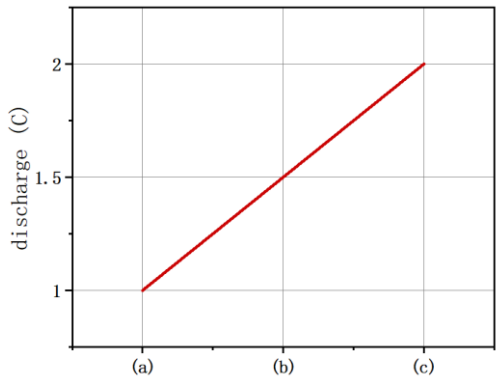

Fig.10 The discharge rate corresponding to each experiment.

4. Conclusions

In this study, MIL-101(Cr) was prepared by high-speed centrifugation, and MIL-101(Cr) was verified by SEM, XRD, BET tests, and the combination of MIL-101(Cr) and MHPA was used in the thermal management of the battery pack to verify the cooling effect of MHPA@MIL-101(Cr) with the increase of the number of cells at different charging rates. The main conclusions were as follows:

1) High-purity MIL-101(Cr) was synthesized by multiple high-speed centrifugations. The micropore diameter was 1.2-3.5nm and the mesopore diameter was 13-23nm. The water vapor adsorption capacity reached 1.65g/g, which had a good water vapor adsorption capacity.

2) The combination of MIL-101(Cr) and MHPA in the thermal management of the battery pack provided significant cooling compared to natural cooling. At a discharge rate of 2C, the maximum temperature of the battery pack of one battery was reduced by 9.78°C, and the battery pack of two cells was reduced by 11.22°C.

3) When the number of cells reached 4, the maximum temperature and temperature difference of the battery pack under the condition of 2C discharge has exceeded the safe temperature range. The experiment was divided into three control groups: natural cooling, MHPA, MHPA@MIL-101(Cr), and the discharge experiments of 1C, 1.5C and 2C were carried out in the battery pack composed of four cells. From the experimental data, it can be seen that with the increase of discharge rate, the maximum temperature of the MHPA@MIL-101(Cr) group rose from 36.42°C to 42.75°C and finally to 47.37°C, and the temperature difference rose from 2.87°C to 3.95°C and finally to 5.57°C, which is beyond the safe temperature range. The results show that when the number of cells in the battery pack is large and the discharge rate is large, the passive cooling method of MOF and MHPA alone is not effective, and it still needs to be combined with other thermal management methods of active cooling.

Acknowledgement

The authors gratefully acknowledge the financial supports from the National Key Research and Development Program of China (2023YFC3008802), the National innovation and entrepreneurship training program for college students (202310497002), and the Key R&D Program of Hubei Province（2023BEB021）.

References

[1] Burdyny, T.,W.A. Smith, CO_2 reduction on gas-diffusion electrodes and why catalytic performance must be assessed at commercially-relevant conditions, *ENERGY & ENVIRONMENTAL SCIENCE*, *12*. (2019), 5, pp. 1442-1453, DOI No. 10.1039/c8ee03134g

[2] Hadjipaschalis, I., *et al.*, Overview of current and future energy storage technologies for electric power applications, *Renewable and sustainable energy reviews*, *13*. (2009), 6-7, pp. 1513-1522

[3] Hall, P.J.,E.J. Bain, Energy-storage technologies and electricity generation, *Energy policy*, *36*. (2008), 12, pp. 4352-4355

[4] Zhu, Z., *et al.*, Rechargeable batteries for grid scale energy storage, *Chemical Reviews*, *122*. (2022), 22, pp. 16610-16751

[5] Wang, Y., *et al.*, Challenges and opportunities to mitigate the catastrophic thermal runaway of high- energy batteries, *Advanced Energy Materials*, *13*. (2023), 15, p. 2203841

[6] Hu, S., *et al.*, A hybrid cooling method with low energy consumption for lithium-ion battery under extreme conditions, *Energy Conversion and Management*, *266*. (2022), p. 115831

[7] Hasani, A.H., *et al.*, Thermal behavior of lithium-ion battery in microgrid application: Impact and management system, *International Journal of Energy Research*, *45*. (2021), 4, pp. 4967-5005, DOI No. 10.1002/er.6229

[8] Mallick, S.,D. Gayen, Thermal behaviour and thermal runaway propagation in lithium-ion battery systems–A critical review, *Journal of Energy Storage*, *62*. (2023), p. 106894

[9] Hailu, G., *et al.*, Stationary battery thermal management: analysis of active cooling designs, *Batteries*, *8*. (2022), 3, p. 23

[10] Thakur, A.K., *et al.*, A state-of-the art review on advancing battery thermal management systems for fast-charging, *Applied Thermal Engineering*, *226*. (2023), p. 120303

[11] Lin, J., *et al.*, Novel battery thermal management via scalable dew-point evaporative cooling, *Energy Conversion and Management*, *283*. (2023), p. 116948

[12] Xie, N., *et al.*, Thermal performance and structural optimization of a hybrid thermal management system based on MHPA/PCM/liquid cooling for lithium-ion battery, *Applied Thermal Engineering*, *235*. (2023), p. 16, DOI No. 10.1016/j.applthermaleng.2023.121341

[13] Zeng, W., *et al.*, Cooling performance and optimization of a new hybrid thermal management system of cylindrical battery, *Applied Thermal Engineering*, *217*. (2022), p. 14, DOI No. 10.1016/j.applthermaleng.2022.119171

[14] Weragoda, D.M., *et al.*, A comprehensive review on heat pipe based battery thermal management systems, *Applied thermal engineering*, *224*. (2023), p. 120070

[15] Faghri, A., Review and Advances in Heat Pipe Science and Technology, *Journal of Heat Transfer-Transactions of the Asme*, *134*. (2012), 12, p. 18, DOI No. 10.1115/1.4007407

[16] Wang, S.S., *et al.*, Performance simulation of L-shaped heat pipe and air coupled cooling process for ternary lithium battery module, *Engineering Applications of Computational Fluid Mechanics*, *18*. (2024), 1, p. 18, DOI No. 10.1080/19942060.2023.2301058

[17] Dan, D., *et al.*, Dynamic thermal behavior of micro heat pipe array-air cooling battery thermal management system based on thermal network model, *Applied Thermal Engineering*, *162*. (2019), p. 114183

[18] Luo, J., *et al.*, Battery thermal management systems (BTMs) based on phase change material (PCM): A comprehensive review, *Chemical Engineering Journal*, *430*. (2022), p. 132741

[19] Ma, C.Y., *et al.*, A copper nanoparticle enhanced phase change material with high thermal conductivity and latent heat for battery thermal management, *Journal of Loss Prevention in the Process Industries*, *78*. (2022), p. 9, DOI No. 10.1016/j.jlp.2022.104814

[20] Liu, Y., *et al.*, High latent heat phase change materials (PCMs) with low melting temperature for thermal management and storage of electronic devices and power batteries: Critical review, *Renewable and Sustainable Energy Reviews, 168*. (2022), p. 112783

[21] Huang, Q., *et al.*, Thermal management of Lithium-ion battery pack through the application of flexible form-stable composite phase change materials, *Applied Thermal Engineering, 183*. (2021), p. 116151

[22] Akbarzadeh, M., *et al.*, A novel liquid cooling plate concept for thermal management of lithium-ion batteries in electric vehicles, *Energy Conversion and Management, 231*. (2021), p. 113862

[23] Cai, G., *et al.*, Metal–organic framework-based hierarchically porous materials: synthesis and applications, *Chemical Reviews, 121*. (2021), 20, pp. 12278-12326

[24] Zhao, T., *et al.*, Lattice oxygen-me diate d Co-O-Fe formation in Co-MOF via Fe doping and ligand design for efficient oxygen evolution, *Journal of Materials Science & Technology, 189*. (2024), pp. 183-190, DOI No. 10.1016/j.jmst.2023.11.070

[25] Li, W., *et al.*, Rational design and general synthesis of multimetallic metal–organic framework nano- octahedra for enhanced Li–S battery, *Advanced Materials, 33*. (2021), 45, p. 2105163

[26] Nabi, S., *et al.*, Metal-organic framework functionalized sulphur doped graphene: a promising platform for selective and sensitive electrochemical sensing of acetaminophen, dopamine and H₂O₂, *New Journal of Chemistry, 46*. (2022), 4, pp. 1588-1600, DOI No. 10.1039/d1nj04041c

[27] Li, W.Y., *et al.*, A novel Ni/Co metal-organic framework with a porous organic polymer material as a ligand for a high-performance supercapacitor and a glucose sensor, *New Journal of Chemistry, 46*. (2022), 47, pp. 22849-22861, DOI No. 10.1039/d2nj04080h

[28] Rani, P.,R. Srivastava, Tailoring the catalytic activity of metal organic frameworks by tuning the metal center and basic functional sites, *New Journal of Chemistry, 41*. (2017), 16, pp. 8166-8177, DOI No. 10.1039/c7nj01055a

[29] Rim, G., *et al.*, Sub-Ambient Temperature Direct Air Capture of CO2 using Amine-Impregnated MIL-101(Cr) Enables Ambient Temperature CO2 Recovery, *JACS Au, 2*. (2022), 2, pp. 380-393, DOI No. 10.1021/jacsau.1c00414

[30] Wang, C., *et al.*, A thermal management strategy for electronic devices based on moisture sorption-desorption processes, *Joule, 4*. (2020), 2, pp. 435-447

[31] Xu, J., *et al.*, Near-zero-energy smart battery thermal management enabled by sorption energy harvesting from air, *ACS central science, 6*. (2020), 9, pp. 1542-1554

[32] Tao, Y., *et al.*, High-performance and long-term thermal management material of MIL-101Cr@ GO, *Materials Today Physics, 22*. (2022), p. 100572

[33] Yue, Q., *et al.*, A passive thermal management system with thermally enhanced water adsorbents for lithium-ion batteries powering electric vehicles, *Applied Thermal Engineering, 207*. (2022), p. 118156

[34] Hu, S., *et al.*, Efficient purification of metal-organic framework and its trigger strategy in battery thermal management system, *Energy Conversion and Management*, *292*. (2023), p. 117416

[35] Liu, X., *et al.*, Hierarchically porous composite fabrics with ultrahigh metal–organic framework loading for zero-energy-consumption heat dissipation, *Science Bulletin*, *67*. (2022), 19, pp. 1991-2000

[36] Yoo, D.K., *et al.*, Polyaniline-loaded metal-organic framework MIL-101(Cr): Promising adsorbent for CO2 capture with increased capacity and selectivity by polyaniline introduction, *Journal of CO2 Utilization*, *28*. (2018), pp. 319-325

Submitted: 6.07.2024.

Revised: 2.09.2024.

Accepted: 12.10.2024.